

Multiple-band-edge quantum-well intermixing in the InGaAs/InGaAsP/InGaP material system

Erik J. Skogen^{a)} and Larry A. Coldren

Electrical and Computer Engineering Department, University of California, Santa Barbara, California 93106

James W. Raring and Steven P. DenBaars

Materials Department, University of California, Santa Barbara, California 93106

(Received 6 December 2004; accepted 4 May 2005; published online 9 June 2005)

The development of photonic integrated circuits lattice matched to GaAs are desirable for the manufacture of high-power, high-efficiency optical components. In this letter we investigate and describe a process technique based on quantum-well intermixing to achieve multiple band edges in the Al-free 980 nm InGaAs/InGaAsP/InGaP material system. © 2005 American Institute of Physics. [DOI: 10.1063/1.1946903]

As the InP- and GaAs-based optoelectronics field matures, it is desirable to monolithically integrate multiple components onto a single chip. These photonic integrated circuits (PICs) will allow for reduced cost, improved performance, and increased functionality over discrete components. The realization of an optimally performing PIC is the primary challenge, as each integrated component requires differing materials and architectural features based on its specific function, and to do so is technologically difficult.

Selective area quantum-well intermixing (QWI) has been shown to be a promising method of tailoring the quantum-well band edge in optoelectronic devices. There have been reports of complex PICs fabricated using selective QWI in the InP material system.¹⁻³

This work focuses on QWI in the GaAs material system. In the past, many 980 nm components made use of InGaAs/GaAs/AlGaAs-based structures, and there have been many reports of achieving QWI in such active regions.^{3,4} However, InGaAs/InGaAsP/InGaP-based devices offer numerous advantages over the InGaAs/GaAs/AlGaAs based devices.^{5,6} For instance, the InGaAsP material has a direct band gap throughout its compositional range, donor related DX centers are not as significant as in AlGaAs, and the reliability may also be improved due to the absence of dark line defects and catastrophic mirror facet damage due to oxidation. Fundamental improvements in the carrier confinement in the quantum wells have been observed in InGaAs/InGaAsP active regions over InGaAs/GaAs active regions, leading to increased differential efficiency and improved thermal characteristics of lasers.⁶ The InGaAs/InGaAsP/InGaP-based devices are also more desirable from an integration standpoint as the selective wet chemical etching of InGaP over GaAs allows for simple process techniques. Furthermore, exposed surfaces utilizing materials with minimal tendency for oxidation are well suited for epitaxial regrowths.

It is shown that multiple-quantum-well (MQW) active regions based on an InGaAs/InGaAsP constant-*x* design are more stable at elevated temperatures than those comprised of

an InGaAs/GaAs constant-*y* design when subjected to impurity-free vacancy diffusion (IFVD) using plasma-enhanced chemical vapor deposited SiO_xN_y. This suggests that the intermixing employing the IFVD method using a dielectric cap is occurring largely on the group-III sublattice. When InGaAs/InGaAsP MQW active regions are subjected to ion-implantation-enhanced QWI, we show that intermixing occurs, suggesting that point defects generated during the implant are capable of interdiffusing on the group-V sublattice. It is also shown that multiple band edges across the wafer can be achieved using a cyclic etch and anneal process, a result similar to that previously reported in InP material system.¹

In this experiment, five epitaxial base structures were grown each with different combinations of MQW and implant buffer layer, as shown in Fig. 1. The base structures were grown using a Thomas Swan Scientific Equipment Ltd. horizontal-flow rotating-disk metalorganic chemical vapor deposition (MOCVD) system on (100) GaAs misoriented 2° towards <111>A. The MQW regions were composed of 8- or 9-nm InGaAs quantum wells (In=0.185) and either GaAs or 0.76Q (InGaAsP λ_g=0.76 μm) tensile strained 0.15% barriers 10 or 11 nm thick. In the case of the InGaAs/InGaAsP MQW the structure is a constant-*x* design. That is, the same

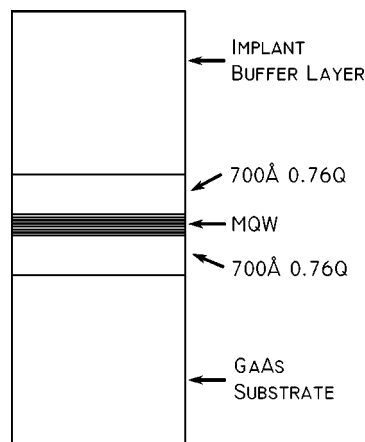


FIG. 1. Epitaxial base structure with either (InGaAs/InGaAsP) MQW or (InGaAs/GaAs) MQW active region, and GaAs or InGaP implant buffer layer.

^{a)} Author is now with Sandia National Laboratories, P.O. Box 5800 MS 0603, Albuquerque, New Mexico 87185-0603; electronic mail: ejskoge@sandia.gov

TABLE I. Epitaxial base structures used in the intermixing experiments. Samples A through D use an implant buffer layer thickness of 200 nm; sample E uses a 500 nm implant buffer layer. Samples A through D use a MQW consisting of 9-nm wells and 11-nm barriers, while sample E uses 8-nm wells and 10-nm barriers.

Sample	MQW	Implant buffer layer
A	InGaAs/GaAs	GaAs
B	InGaAs/GaAs	InGaP
C	InGaAs/InGaAsP	GaAs
D	InGaAs/InGaAsP	InGaP
E	InGaAs/InGaAsP	InGaP

group-III composition is used in the wells and barriers. The MQW was centered within a symmetric waveguide structure consisting of 70 nm of 0.76Q on either side of the MQW. An implant buffer layer was grown above the structure and designed to capture the ion implant, creating point defects above the active region, and consisted of either 200 nm GaAs, 200 nm of InGaP, or 500 nm of InGaP. In those base structures using the InGaP implant buffer layers, the implant buffer layer can be selectively removed. The base structures are summarized in Table I.

The samples were cleaved and a portion of each was ion implanted. Phosphorus was implanted at an energy of 100 keV and a dose of $2 \times 10^{14} \text{ cm}^{-2}$, the implant was carried out at a temperature of 200 °C, yielding a range of 110 nm in InGaP and 93 nm in GaAs. Both implanted and nonimplanted samples were encapsulated with 40 nm of SiO_xN_y to protect the sample surface and subjected to rapid thermal processing for various temperatures and times ranging from 650 to 900 °C, and 15 to 180 s, respectively. The SiO_xN_y was removed using buffered HF and the wavelength of the MQW emission measured using room-temperature photoluminescence with a pump wavelength of 785 nm.

The peak photoluminescence wavelength shifts for samples that are not implanted are plotted as a function of rapid thermal anneal (RTA) temperature, shown in Fig. 2. The RTA time for these samples is 120-seconds. This demonstrates the temperature at which interfaces that have dielectric caps, yet have not been subjected to the implantation process, begin to interdiffuse. The two samples, which use an InGaAs/GaAs MQW, show an appreciable shift in the quan-

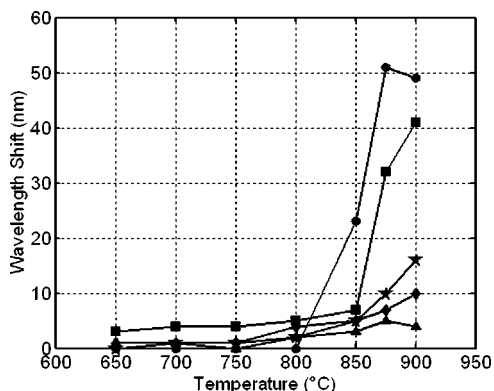


FIG. 2. Photoluminescence peak wavelength shift vs RTA temperature for nonimplanted base structures. Sample A (InGaAs/GaAs) MQW with a GaAs cap (circles), sample B (InGaAs/GaAs) MQW with a InGaP cap (triangles), sample C (InGaAs/InGaAsP) MQW with a GaAs cap (diamonds), sample D (InGaAs/InGaAsP) MQW with an InGaP cap (stars), and sample E (InGaAs/InGaAsP) MQW with a 500 nm InGaP cap (squares).

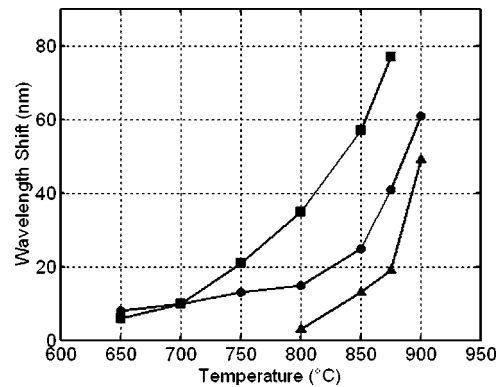


FIG. 3. Photoluminescence peak wavelength shift vs RTA temperature for implanted base structures. Sample D (InGaAs/InGaAsP) MQW with a 200 nm InGaP cap (circles), sample E (InGaAs/InGaAsP) MQW with a 500 nm InGaP cap (squares), and sample E with an InGaP cap removed prior to annealing (triangles).

tized energy state within the temperature range tested. In contrast, the samples which employ an InGaAs/InGaAsP MQW do not shift to such an extent.

The photoluminescence peak wavelength shifts of samples subjected to implantation are shown in Fig. 3. The RTA time for these samples was again 120 s. The photoluminescence response of the samples that incorporate a GaAs implant buffer layer are not visible due to the damage from the implant in the GaAs layer, thereby blocking the photoexcited carriers from reaching the MQW, whereas for the samples with an InGaP cap the photoluminescence signal is present because the photocarriers are generated at the MQW due to the fact that InGaP is transparent at the pump wavelength. For this reason, only those samples that utilize an InGaP implant buffer layer are shown. Furthermore, it is only those samples that use the InGaAs/InGaAsP MQW that are stable at elevated temperatures when encapsulated with SiO_xN_y , and are of interest; therefore, only samples employing the InGaAsP barriers are shown, samples D and E. Sample D uses a 200 nm InGaP implant buffer layer, while sample E uses a 500 nm InGaP implant buffer layer. Also shown in Fig. 3 is the photoluminescence peak wavelength shift of sample E, which has been implanted, and had the implanted InGaP buffer layer etched away prior to annealing.

All heterointerfaces are metastable by nature, and with enough input energy compositional gradients will interdiffuse without the need for a catalyst. For conservation of the as-grown MQW, it is essential that sharp heterointerfaces remain intact at elevated temperatures. As demonstrated in Fig. 2, the samples using InGaAs/GaAs MQWs have a tendency to interdiffuse at lower temperatures than those samples that use InGaAs/InGaAsP MQWs. This is due to the introduction of group-III vacancies at the sample/dielectric interface which have a tendency to interdiffuse species residing on the group-III sublattice only.⁷ In the case of the InGaAs/GaAs MQW the intermixing takes place on the group-III sublattice, while in the InGaAs/InGaAsP MQWs, because the same group-III composition is used in the wells and barriers the compositional gradient is only on the group-V sublattice and therefore remains intact in the presence of group-III vacancies. Therefore, we conclude that the group-V sublattice is more stable and less likely to interdiffuse at elevated temperatures than the group-III sublattice in samples encapsulated by SiO_xN_y .

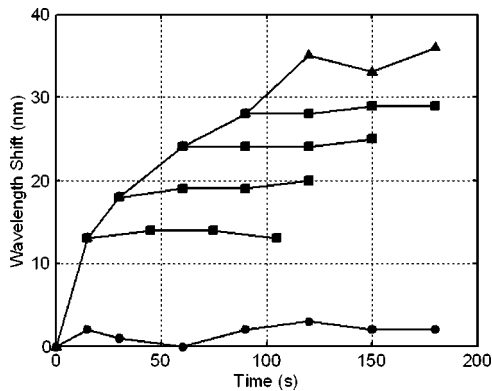


FIG. 4. Isothermal, 800 °C, photoluminescence peak wavelength shift as a function of RTA time demonstrating multiple band edges using a single-ion implant. Symbols indicate nonimplanted (circles), implanted (triangles), and samples with partial anneal followed by the removal of the implant buffer layer (squares) followed by further anneals.

When considering the implanted structures, it is clear that the InGaAs/InGaAsP MQWs readily interdiffuse due to the introduction of point defects that are created in the InGaP layer during implantation. A more substantial shift of the photoluminescence peak wavelength is observed in sample E, a 500 nm thick implant buffer layer, than observed for sample D, a 200 nm thick implant buffer layer. The origin of the difference is not understood at this time, however, we speculate that the proximity of the implant to the MQW and/or strain in the implant buffer layer could play a role. Nevertheless, the transport of point defects through InGaP is readily achievable in either structure.

An important aspect of the implant enhanced intermixing is the extent to which the wells and barriers interdiffuse once the implant buffer layer is removed. A lack of blueshift of the emission wavelength implies the MQW will be stable during future high-temperature processing, such as further anneals and MOCVD regrowth. As shown in Fig. 3, significant intermixing begins to occur at 850 °C for the sample with the implant buffer layer removed. Thus, in order to ensure the MQW will not interdiffuse, the anneal temperature should be kept below 850 °C.

With this information, it is possible to construct a process for the achievement of multiple band edges across the wafer using a single implantation process. This process is demonstrated in Fig. 4, where isothermal annealing at 800 °C was performed for various times. Both implanted and nonimplanted samples were annealed for times ranging from 15 to 180 s, as shown in the figure. After the 15, 30, 60, and 90 second anneals, the implant buffer layer was removed from the respective samples. These samples were then subjected to additional anneal cycles. We found that

removing the implant buffer layer halted the blue-shift during these anneals. The arrest of the blueshift is the result of the removal of the abundance of point defects which reside in the implant buffer layer, which are necessary for intermixing. With this process it is possible to achieve any number of band edges across the wafer, limited only by the practical number of lithographic process steps.

Implantation-enhanced QWI in the GaAs material system has been investigated. Several combinations of MQW and implant buffer layer have been studied. It was found that constant- x InGaAs/InGaAsP MQWs are more stable at elevated temperatures than InGaAs/GaAs MQWs when encapsulated with SiO_xN_y . This supports the fact that interdiffusion occurs more readily on the group-III sublattice than on the group-V sublattice in the presence of group-III vacancies. This stability is desirable for the development of a selective QWI process.

Significant interdiffusion enhancement in the InGaAs/InGaAsP was achieved using ion implantation into an InGaP implant buffer layer followed by rapid thermal processing. It was found that point defects readily diffuse through the InGaP allowing for intermixing to occur in the MQW. The ability for the InGaAs/InGaAsP MQW to remain stable without the introduction of point defects, while readily diffusing when point defects are present make this material system ideal for the development of a selective QWI process.

A selective QWI process was developed and demonstrated using a sacrificial implant buffer layer. Using a single-ion implant, multiple band edges can be achieved by ceasing the anneal prior to the saturation of blue-shift, removing the implant buffer layer in those regions where the desired blueshift has been reached, and continuing the anneal. In those regions where the implant buffer layer was removed, the blueshift was halted, whereas in those regions the implant buffer layer remained the intermixing continued. This result shows the feasibility of creating high-performance PICs in this material system.

¹E. Skogen, J. Raring, J. Barton, S. DenBaars, and L. Coldren, *IEEE J. Sel. Top. Quantum Electron.* **9**, 1183 (2003).

²S. McDougall, O. Kowalski, C. Hamilton, F. Camacho, B. Qiu, M. Ke, R. De La Rue, A. Bryce, and J. Marsh, *IEEE J. Sel. Top. Quantum Electron.* **4**, 636 (1998).

³S. Charbonneau, E. Kotels, P. Poole, J. He, G. Aers, J. Haysom, M. Buchanan, Y. Feng, A. Delage, F. Yang, M. Davies, R. Goldberg, P. Piva, and I. Mitchell, *IEEE J. Sel. Top. Quantum Electron.* **4**, 772 (1998).

⁴A. Helmy, J. Aitchison, and J. Marsh, *Appl. Phys. Lett.* **71**, 2998 (1997).

⁵M. Ohjubo, S. Namiki, T. Ijichi, A. Iketani, and T. Kikuta, *IEEE J. Quantum Electron.* **29**, 1932 (1993).

⁶G. Zhang, A. Ovtchinnikov, J. Nappi, H. Asonen, and M. Pessa, *IEEE J. Quantum Electron.* **29**, 1943 (1993).

⁷A. Helmy, J. Aitchison, and J. Marsh, *IEEE J. Sel. Top. Quantum Electron.* **4**, 653 (1998).